NIH Public Access
Author Manuscript
Gene Expr Patterns. Author manuscript; available in PMC 2010 July 2.

Published in final edited form as:
Gene Expr Patterns. 2010 June ; 10(4-5): 159–166. doi:10.1016/j.gep.2010.04.004.

Expression analysis of Runx3 and other Runx family members during *Xenopus* development

Byung-Yong Park[1,2] and **Jean-Pierre Saint-Jeannet**[2,*]

[1]Department of Anatomy, College of Veterinary Medicine, Chonbuk National University, Jeonju, Jeonbuk 561-756, Republic of Korea

[2]Department of Animal Biology, School of Veterinary Medicine, University of Pennsylvania, 3800 Spruce Street, Philadelphia, PA 19104, USA

Abstract

Runx genes encode a family of proteins defined by the highly conserved Runt DNA-binding domain. Studies in several organisms have shown that these transcription factors regulate multiple aspects of embryonic development and are responsible for the pathogenesis of several human diseases. Here we report the cloning and expression of *Runx3* during *Xenopus* development and compare its expression pattern to other Runx family members, *Runx1* and *Runx2*, and to *Cbf*β, the obligatory binding-partner of Runx proteins. Using in situ hybridization in the whole embryo and on sections we show that *Runx3* is co-expressed with *Runx1* in the hematopoietic lineage and in Rohon-Beard sensory neurons. In contrast *Runx3* and *Runx2* are co-expressed in craniofacial cartilage elements. *Runx3* shows also unique expression domains in a number of derivatives of the neurogenic placodes, including the ganglia of the anteroposterior and middle lateral line nerves, and ganglia of the trigeminal, glossopharyngeal, facial and vagal nerves. These observations suggest a critical role for *Runx3* in the development of cranial sensory neurons, while in other tissues its co-expression with *Runx1* or *Runx2* may signify functional redundancy between these family members.

Keywords

Xenopus; Runx1; Runx2; Runx3; Cbfβ; Islet1; Pax3; Placode; Cartilage; Craniofacial; Rohon-Beard neuron; Cranial nerve; Trigeminal; Profundal; Vagal; Glossopharyngeal; Lateral line

1. Results and Discussion

Runx3, also known as Aml2/Cbfα3/Pebp2αC, belongs to the Runx family of transcription factors, which include Runx1 (Aml1/Cbfα2/Pebp2αB) and Runx2 (Aml3/Cbfα1/Pebp2αA). This class of molecules is defined by the presence of the runt domain, a highly conserved DNA binding and protein-protein interaction domain. Runx proteins bind DNA in association with the non-DNA-binding partner, Cbfβ, that confers high-affinity DNA binding and stability to the complex. This heterodimeric complex has the ability to activate or repress transcription of key regulators of cell growth, proliferation, survival and differentiation (reviewed in Blyth et al., 2005; Ito, 2008).

The function of the three mammalian *Runx* genes has been studied using gene-targeting technology in the mouse. *Runx1* is primarily required for hematopoiesis and is essential for the

*Correspondence: Jean-Pierre Saint-Jeannet, Department of Animal Biology, School of Veterinary Medicine, University of Pennsylvania, 3800 Spruce Street, Philadelphia, PA 19104, Tel: 215-898-1666, Fax: 215-573-5186, saintj@vet.upenn.edu.

NIH-PA Author Manuscript
NIH-PA Author Manuscript
NIH-PA Author Manuscript

NIH-PA Author Manuscript

NIH-PA Author Manuscript

NIH-PA Author Manuscript

generation of hematopoietic stem cells (Okuda et al., 1996; Wang et al., 1996; North et al., 1999). *RUNX1* is a frequent target of gene rearrangements and mutations in a spectrum of human leukemias including acute myeloid leukemia (Speck and Gilliland, 2002). *Runx2* is required for bone development and is associated with human cleidocranial dysplasia, a skeletal disorder characterized by bone and dental abnormalities (Komori et al., 1997; Otto et al., 1997; Mundlos et al., 1997). *Runx3* is expressed in a broader range of tissues compared to the other two *Runx* genes, and has been implicated in development of axonal projections of a subpopulation of neurons in the dorsal root ganglia (Levanon et al., 2002; Inoue et al., 2002) and in the formation of the gastrointestinal tract (Li et al., 2002). There is also evidence that Runx3 functions as a tumor suppressor in gastric cancers (Li et al., 2002; Brenner et al., 2004).

The expression and function of *Runx* genes has been relatively well conserved during evolution. For example, in zebrafish and *Xenopus Runx1* is expressed in blood progenitors, and controls hematopoietic stem cell specification (Tracey et al., 1998; Kalev-Zylinska et al., 2002; Burns et al., 2005). *Runx2* in fish and frogs is detected in developing skeletal elements where it regulates chondrogenesis (Flores et al., 2004; 2006; Kerney et al., 2007). Zebrafish *runx3* is expressed in hematopoietic, neuronal and cartilaginous tissues and its function has been studied in the context of hematopoiesis (Kalev-Zylinska et al., 2003) and chondrocyte differentiation (Flores et al., 2006). Here we report the cloning of *Xenopus Runx3* and provide a comprehensive analysis of *Runx3* expression during *Xenopus* embryogenesis, comparing its expression pattern to that of *Runx1*, *Runx2* and *Cbf*β.

1.1. Cloning of *Xenopus laevis Runx3*

A PCR product corresponding to a partial sequence of the *Xenopus laevis Runx3* open reading frame was amplified from stage 30 embryonic cDNA using primers designed based on *Xenopus tropicalis Runx3* sequence. The complete coding region of *Xenopus laevis Runx3* was subsequently established by two rounds of PCR using stage 41 embryonic cDNA and based on the sequence of *Xenopus tropicalis Runx3*. *Xenopus laevis Runx3* possesses an open reading frame encoding 393 amino acids (Fig. 1A). At the amino acid level, *Xenopus laevis Runx3* shares 76% identity with human *RUNX3* (Levanon et al., 1994), 74% identity with mouse *Runx3* (Wijmenga et al., 1995) and 65% identity with zebrafish *runx3* (Kataoka et al., 2000;Burns et al., 2002). When compared to *Xenopus laevis Runx1/Xaml1* (Tracey et al., 1998) and *Xenopus laevis Runx2* (Kerney et al., 2007), the overall amino acid identity drops to 55% and 56%, respectively. Assignment of *Xenopus laevis Runx3* sequence to the Runx family was based on phylogenetic tree analysis of the predicted amino acid sequences compared to that of selected vertebrate species (Fig 1B). This analysis indicates that *Xenopus laevis Runx3* represents an ortholog of mammalian *Runx3*.

1.2. Temporal expression of *Runx3* and other *Runx* family members

To determine the temporal expression of *Runx3* we performed RT-PCR of embryonic RNA at different stages of development. We also compared *Runx3* expression profile to that of *Runx1*, *Runx2* and *Cbf*β (Fig 2A). These results were independently confirmed by real-time RT-PCR (Fig 2B). *Runx3* is first detected around stage 20, while *Runx1* transcription is initiated before stage 10, consistent with previous work (Tracey et al., 1998). *Runx1* and *Runx3* transcripts persist at least up to stage 40, the latest stage analyzed in this study. *Runx2* and *Cbf*β are both maternally expressed, and while *Cbf*β is expressed at all stages examined, *Runx2* exhibits a dramatic down regulation between stage 10 (gastrula) and stage 29/30 (tailbud). The biphasic temporal expression profile of *Runx2* has not been previously described in *Xenopus* (Kerney et al., 2007), presumably because we have analyzed a broader range of embryonic stages here than in previous work. In zebrafish *runx2b type2* follow a very similar expression profile, with the maternal component detected in the early zygote, followed by a

NIH-PA Author Manuscript

NIH-PA Author Manuscript

NIH-PA Author Manuscript

reduction in expression levels by 6 hpf, and a phase of upregulation around 18 hpf, corresponding to the zygotic expression (Flores et al., 2008).

1.3. Comparative analysis of *Runx3*, *Runx1*, *Runx2* and *Cbf*β expression

1.3.1 Whole-mount in situ hybridization analysis—To determine the expression pattern of *Runx3*, we performed whole-mount *in situ* hybridization on embryos at different stages of development (Fig 3; Fig 4A). Antisense and control sense probes were analyzed to established specificity of the signal for each gene (control sense hybridization, not shown). *Runx3* transcripts are first detected at stage 20 in two domains, the developing primary sensory (Rohon-Beard) neurons in the dorsal spinal cord and the profundal-trigeminal placode, which appear as bilateral clusters of cells posterior to the eye primordia (Fig 3). At the same stage *Runx1* is also expressed in Rohon-Beard sensory neurons, as well as in the ventrally located blood progenitors (Fig 3). *Runx1* can be detected in both of these domains as early as stage 13 (Fig 3 and not shown), as previously reported (Tracey et al., 1998). *Runx3* is also detected in the hematopoietic progenitors but not until stage 31, in a pattern that overlaps with *Runx1* and *Cbf*β at least in the lateral most aspect of the lateral plate mesoderm (Fig 4). The apparent difference in the expression of these genes in the hematopoietic lineage may reflect differences in the expression level of these molecules, *Runx1* being more strongly expressed than *Runx3* and *Cbf*β at the ventral midline (Fig 4). The obligatory partner of all Runx proteins, *Cbf*β, is detected in the same three domains as *Runx3* and *Runx1* (Fig 3 and Fig 4). *Cbf*β expression in blood progenitors is first detected at stage 22 (not shown) several hours after *Runx1* onset of expression in this lineage (Fig 3). *Cbf*β expression at stage 13 is expressed at the neural plate border in a pattern reminiscent to that of *Pax3*, and more broadly than the expression domain of *Runx1* in Rohon-Beard sensory neurons. At later stages, stage 25 and up, *Runx3* expression appears to be largely confined to the head region and in a number of cranial nerves including the ganglia of the trigeminal, vagal and glossopharyngeal nerves, where it overlaps with *Cbf*β (Fig 3). *Runx2* is first detected around stage 35/36 in the developing craniofacial structures as previously described (Kerney et al., 2007). To confirm the tissue-specific expression analysis of the *Runx* genes, we also performed *in situ* hybridization for *Pax3* and *Islet1* in staged matched embryos (Fig 3). These two genes share common expression domains with *Runx* genes in the profundal-trigeminal placode (*Pax3* and *Islet1*), Rohon-Beard sensory neurons and cranial ganglia (*Islet1*). In zebrafish *Runx3* is expressed in the same four domains: hematopoietic lineage, trigeminal ganglia, Rohon-Beard neurons and cartilaginous tissues in the head (Kalev-Zylinska et al., 2003). While *Runx3* has been reported to be expressed in the mouse gastrointestinal tract (Li et al., 2002), and in zebrafish intestinal bulb (Kalev-Zylinska et al., 2003), we could not detect *Runx3* expression in the developing gut at the stages examined, though we cannot exclude that it is expressed in this lineage later in development.

Next we undertook a detailed analysis of *Runx3* expression using *in situ* hybridization on sections at stage 20 and 40, focusing on the early expression of *Runx3* in the profundal-trigeminal placode and Rohon-Beard sensory neurons (Fig 5), and its later expression in the branchial arches (Fig 6) and derivatives of the neurogenic placodes (Fig 7).

1.3.2 *Runx3* expression in profundal-trigeminal placode and Rohon-Beard sensory neurons at stage 20—The profundal and trigeminal placodes are initially fused into a single profundal-trigeminal complex located immediately dorsal and posterior to the developing eye. These placodes give rise to neurons of the profundal and trigeminal nerves, respectively (Schlosser and Northcutt, 2000). To confirm the expression of *Runx3* in this domain we also analyzed *Islet1* expression in staged matched embryos. We found that *Runx3* and *Islet1* are co-expressed in this placode, however unlike *Islet1*, which is expressed in the entire placodal domain, *Runx3* and *Cbf*β are detected only a sub-region of this developing placode (Fig 5 A-C).

NIH-PA Author Manuscript

NIH-PA Author Manuscript

NIH-PA Author Manuscript

Lower vertebrates develop a unique set of primary sensory neurons located in the dorsal spinal cord. These cells, known as Rohon-Beard sensory neurons, innervate the skin and are critical to mediate the escape response to touch during larval stages (Roberts, 2000). Later in development, these neurons undergo apoptosis and are replaced by the neural crest-derived dorsal root ganglia neurons. *Runx3* is detected in Rohon-Beard sensory neurons and this expression appears to overlap with that of *Islet1*, *Runx1* and *Cbf*β in these cells (Fig 5D). *Islet1* is also detected in a second row of primary neurons that will give rise to interneurons, located ventral to the row of Rohon-Beard neurons (Fig 5D). To confirm the co-expression of these genes in Rohon-Beard sensory neurons we performed in situ hybridization on adjacent sections of the same embryo alternating in situ probes. We found that while *Runx3* is only expressed in a subset of Rohon-Beard neurons (Fig 1S), it is co-expressed in these cells with *Cbf*β, *Runx1* and *Islet1* (Fig 1S). *Runx1*, *Islet1* and *Cbf*β appear to be co-expressed in the entire population of Rohon-Beard neurons (Fig 1S), although each one with slightly different onset of expression (not shown).

1.3.3 *Runx3* expression in craniofacial cartilage at stage 40—Whole-mount *in situ* hybridization indicates that *Runx3* is expressed in the branchial arches starting at stage 35/36 and is co-expressed in this domain with *Runx2* and *Cbf*β. To determine the specific cartilage elements in which *Runx3* is expressed, we performed *in situ* hybridization on serial sections of stage 40 embryos. Cartilage elements (Fig 6A-C) were identified based on the nomenclature of Sadaghiani and Thiebaud (1987). With the exception of the basihyal *Runx2* is detected in all cartilage elements (Fig 6D-H). *Runx3* on the other hand is expressed in the basihyal cartilage in addition to the Meckel's, ceratoyal, and ethmoid-trabecular cartilages (Fig 6D-H). *Runx1* is detected in a few scattered cells within the ceratohyal cartilage (Fig 6F) and in the pharyngeal endoderm overlying the developing branchial cartilages (Fig 6H). This is in contrast to what has been reported in Zebrafish where *runx3* is expressed in the pharyngeal endoderm (Kalev-Zylinska et al., 2003;Flores et al., 2006). As expected, *Cbf*β is uniformly expressed in all cartilage elements (Fig 6D-H). Co-expression of *Runx2* and *Runx3* in the developing cartilage is conserved in zebrafish, chick and mouse embryos (Flores et al., 2006;Stricker et al., 2002).

1.3.4 *Runx3* expression in neurogenic placode derivatives at stage 40— Neurogenic placodes in *Xenopus laevis* comprise the olfactory placode, the profundal and trigeminal placodes, a series of epibranchial placodes, two hypobranchial placodes, the otic placode, and five lateral line placodes (Schlosser and Northcutt, 2000). To precisely evaluate the expression of *Runx3* in the derivatives of these placodes we also analyzed the expression of *Islet1* a gene expressed in all cranial ganglia and nerves (Brade et al., 2007). We performed sections at three different levels along the anteroposterior axis focusing on the pre-otic, otic and post-otic regions.

In the pre-otic region *Runx3* is expressed in the ganglia of the trigeminal, anterodorsal lateral line nerves and the fused ganglia of the facial and anteroventral lateral line nerves, though at a lower level in the anterodorsal lateral line ganglion (Fig 7; pre-otic). Ventral to the otic vesicle, *Runx3* is detected in the fused ganglia of the glossopharyngeal and middle lateral line nerves (Fig 7; otic). In this region *Runx1* is expressed in the statoaccoustic ganglia associated with the otic vesicle, where it is coexpressed with *Islet1* (Fig 7; otic). Interestingly, posterior to the otic vesicle, in the fused ganglia of the vagal and posterior lateral line nerves, *Runx1* and *Runx3* have complementary and non-overlapping expression domains. *Runx1* and *Runx3* are restricted to the ganglion of the posterior lateral line nerve and to the ganglion of the vagal nerve, respectively (Fig 7; post-otic). *Runx2* is not detected in any of these ganglia, and *Cbf*β is ubiquitously expressed in all of them (Fig 7).

NIH-PA Author Manuscript

NIH-PA Author Manuscript

NIH-PA Author Manuscript

In summary, *Runx3* is co-expressed with *Runx1* in blood progenitors and Rohon-Beard neurons and with *Runx2* in craniofacial cartilage (Table 1). *Runx3* also has a unique expression domain in a number of derivatives of the neurogenic placodes not shared with other Runx family members, including ganglia of the anteroposterior and middle lateral line nerves, and ganglia of the trigeminal, glossopharyngeal, facial and vagal nerves (Table 1). Our data suggest that Runx3 is an important player in the regulation of cranial sensory neurons development.

2. Experimental Procedures

2.1. Cloning of *Xenopus Runx3*

A partial sequence of the *Xenopus laevis Runx3* ORF was amplified using PCR from stage 30 cDNA using a set of primers designed against two conserved regions of *Runx3* in several species (F: TGCGGAAAGATGGGCGAGAA; R: TCCATTCTTCCAC TAGTGGT) and based on the sequence of *Xenopus tropicalis Runx3* (Ensembl ID, ENSXETT00000002249). The resulting 1100 bp PCR product was purified, subcloned into pGEMTeasy (Promega) and sequenced. This construct is referred as pGEMT-XRunx3. Based on *Xenopus tropicalis* sequence we designed a second set of primers outside *Runx3* ORF (F: AACACCCTGCTGTTGTAATG; R: GGCTGTATTCACAAAG TCTC) to amplify the entire coding region of *Xenopus laevis Runx3*. This product was predicted to include 17 bp of 5'UTR and 20 bp of 3'UTR. The PCR was performed using Taq polymerase and stage 41 cDNA as template. The resulting 1224 bp product was subcloned into pGEMTeasy and multiple clones were sequenced to confirm the sequence of *Xenopus laevis Runx3*. Based on this information, we designed a third set of nested primers (F: ATGCTCATTCCCGTAGACCC; R: TCAATAGGGTCTCCAAA CTG) to amplify the *Xenopus laevis* Runx3 ORF using Pfu polymerase and stage 41 cDNA. The PCR product encoding *Xenopus laevis* Runx3 ORF was subcloned and sequenced. The sequence has been submitted to GeneBank (accession # GU725438).

2.2. Molecular Phylogeny

Multiple sequence alignment of the deduced amino acid sequences of Runx3 was performed using ClustalW (Thompson et al., 1994), and phylogenetic tree was constructed by using the neighbor-joining method (Pearson et al., 1999) through the EMBL–EBI interface (http://www.ebi.ac.uk/Tools/clustalw/). The sequences used in Fig. 1 are human *RUNX1* (NP_001001890), mouse *Runx1* (NP_001104493), chicken *Runx1* (Ensembl ID, ENSGALP00000029722), *Xenopus laevis Runx1* (AAC41269), zebrafish *runx1* (NP_571678), human *RUNX2* (NP_004339), mouse *Runx2* (NP_001139392), chicken *Runx2* (NP_989459), *Xenopus laevis Runx2* (ABM05616), zebrafish *runx2a* (NP_998023), zebrafish *runx2b* (NP_998027), human *RUNX3* (NP_004341), mouse *Runx3* (EDL29993), chicken *Runx3* (XP_001232978) and zebrafish *runx3* (NP_571679).

2.3. RT-PCR analysis

Embryos were staged according to Nieuwkoop and Faber (1967). Total RNA was extracted from embryos at indicated stages using an RNeasy micro RNA isolation kit (Qiagen). To avoid contamination from genomic DNA, the RNA samples were digested with RNase-free DNase I before RT-PCR was performed. RT-PCR experiments were performed using the One Step RT-PCR kit (Qiagen) according to the manufacturer's instructions using the following primer sets: *Runx1* (F: ACTCTGAGTCCGGGGAAGAT; R: CCATATTCCGGTCTGTGCTT; 30 cycles), *Runx2* (F: GCTTCCTGCTATCTCCGA TG; R: GGAGGGCTGTACGTGAATGT; 33 cycles), *Runx3* (F: CACACTGGCCAACAC AAATC; R: TACGAGGGTCGGTAAACCT G; 30 cycles), *Cbf*β (F: GAACGACAAGCA CGTTTTCA; R: CTCCCGTTCAAAGTCCACAT; 26 cycles) and *ODC* (F: ACATGGC ATTCTCCCTGAAG; R: TGGTCCCAAGGCTAAAGTTG; 25 cycles). For real-time RT-PCR the reaction was

NIH-PA Author Manuscript

NIH-PA Author Manuscript

NIH-PA Author Manuscript

performed using the same primer sets and the QuantiTect SYBR Green RT-PCR kit (QIAGEN) on a LightCycler (Roche Diagnostics). The reaction mixture consisted of 10 µl of QuantiTect SYBR Green RT-PCR Master Mix, 500 nM forward and reverse primers, 0.2 µl of RT, and 60 ng of template RNA in a total volume of 20 µl. The cycling conditions were as follow: denaturation at 95°C (3 sec.), annealing at 55°C (4 sec.), and extension at 72°C (12 sec.). By optimizing primers and reaction conditions, a single specific product was amplified as confirmed by melting curve analysis. Each reaction included a control without template and a standard curve of serial dilutions (in 10-fold increments) of test RNAs. In each case, *ornithine decarboxylase* (*ODC*) was used as an internal reference (data not shown). Each bar on the histograms has been normalized to the level of *ODC*.

2.4. *In situ* hybridization

Sense and antisense DIG-labeled probes (Genius kit, Roche) were synthesized using template cDNA encoding *Runx1/Xaml1* (Tracey et al., 1998), *Runx2* (Kerney et al., 2007), *Pax3* (Bang et al., 1997), *Islet1* (Brade et al., 2007), *Cbf*β (Sport6-Cbfβ; Open Biosystems) and *Runx3* (pGEMT-XRunx3). Whole-mount in situ hybridization was performed as described (Harland, 1991). In some cases to ease visualization of the staining embryos were cleared in a mixture of benzyl alcohol and benzyl benzoate (1v:2v). For *in situ* hybridization on sections, embryos at stage 20 and 40 were fixed in MEMFA for 1 hour, embedded in Paraplast and 12 µm sections hybridized with the appropriate probes as described (Henry et al. 1996). Sections were then briefly counter stained with eosin.

Supplementary Material

Refer to Web version on PubMed Central for supplementary material.

Acknowledgments

We thank Drs. Anne Bang, Ryan Kerney, Peter Klein and Petra Pandur for reagents and Dr. Trish Labosky for comments on the manuscript. This work was supported by a grant from the National Institutes of Health to J-P S-J (RO1-DC07175).

References

Bang AG, Papalopulu N, Kintner C, Goulding MD. Expression of Pax-3 is initiatedin the early neural plate by posteriorizing signals produced by the organizer and by posterior non-axial mesoderm. Development 1997;124:2075–2085. [PubMed: 9169853]

Blyth K, Cameron ER, Neil JC. The RUNX genes: Gain or loss of function in cancer. Nat. Rev. Cancer 2005;5:376–387. [PubMed: 15864279]

Brade T, Gessert S, Kühl M, Pandur P. The amphibian second heart field: Xenopus islet-1 is required for cardiovascular development. Dev. Biol 2007;311:297–310. [PubMed: 17900553]

Brenner O, Levanon D, Negreanu V, Golubkov O, Fainaru O, Woolf E, Groner Y. Loss of Runx3 function in leukocytes is associated with spontaneously developed colitis and gastric mucosal hyperplasia. Proc. Natl. Acad. Sci. USA 2004;101:16016–16021. [PubMed: 15514019]

Burns CE, DeBlasio T, Zhou Y, Zhang J, Zon L, Nimer SD. Isolation and characterization of runxa and runxb, zebrafish members of the runt family of transcriptional regulators. Exp. Hematol 2002;30:1381–1389. [PubMed: 12482499]

Burns CE, Traver D, Mayhall E, Shepard JL, Zon LI. Hematopoietic stem cell fate is established by the Notch-Runx pathway. Genes Dev 2005;19:2331–2342. [PubMed: 16166372]

Flores MV, Tsang VW, Hu W, Kalev-Zylinska M, Postlethwait J, Crosier P, Crosier K, Fisher S. Duplicate zebrafish runx2 orthologues are expressed in developing skeletal elements. Gene Expr. Patterns 2004;4:573–581. [PubMed: 15261836]

NIH-PA Author Manuscript

NIH-PA Author Manuscript

NIH-PA Author Manuscript

Flores MV, Lam EYN, Crosier P, Crosier K, Fisher S. A Hierarchy of Runx transcription factors modulate the onset of chondrogenesis in craniofacial endochondral bones in zebrafish. Dev. Dyn 2006;235:3166–3176. [PubMed: 17013873]

Flores MV, Lam EYN, Crosier P, Crosier K. Osteogenic transcription factor Runx2 is a maternal determinant of dorsoventral patterning in zebrafish. Nature Cell Biol 2008;10:346–352. [PubMed: 18246063]

Harland RM. In situ hybridization: an improved whole-mount method for Xenopus embryos. Meth Cell Biol 1991;36:685–695.

Henry GL, Brivanlou IH, Kessler DS, Hemmati-Brivanlou A, Melton DA. TGF-beta signals and a pattern in Xenopus laevis endodermal development. Development 1996;122:1007–1015. [PubMed: 8631246]

Hong C-S, Saint-Jeannet J-P. The activity of Pax3 and Zic1 regulates three distinct cell fates at the neural plate border. Mol. Biol. Cell 2007;18:2192–2202. [PubMed: 17409353]

Inoue K, Ozaki S, Shiga T, Ito K, Masuda T, Okado N, Iseda T, Kawaguchi S, Ogawa M, Bae SC, Yamashita N, Itohara S, et al. Runx3 controls the axonal projection of proprioceptive dorsal root ganglion neurons. Nat. Neurosci 2002;5:946–954. [PubMed: 12352981]

Ito K. RUNX Genes in Development and cancer: regulation of viral gene expression and the discovery of RUNX family genes. Adv. Cancer Res 2008;99:33–76. [PubMed: 18037406]

Kalev-Zylinska ML, Horsfield JA, Flores MV, Postlethwait JH, Vitas MR, Baas AM, Crosier PS, Crosier KE. Runx1 is required for zebrafish blood and vessel development and expression of a human RUNX1-CBF2T1 transgene advances a model for studies of leukemogenesis. Development 2002;129:2015–2030. [PubMed: 11934867]

Kalev-Zylinska ML, Horsfield JA, Flores MV, Postlethwait JH, Chau JY, Cattin PM, Vitas MR, Crosier PS, Crosier KE. Runx3 is required for hematopoietic development in zebrafish. Dev. Dyn 2003;228:323–336. [PubMed: 14579373]

Kataoka H, Ochi M, Enomoto K, Yamaguchi A. Cloning and embryonic expression patterns of the zebrafish Runt domain genes, runxa and runxb. Mech. Dev 2000;98:139–143. [PubMed: 11044618]

Kerney R, Gross JB, Hanken J. Runx2 is essential for larval hyobranchial cartilage formation in Xenopus laevis. Dev. Dyn 2007;236:1650–1662. [PubMed: 17474117]

Komori T, Yagi H, Nomura S, Yamaguchi A, Sasaki K, Deguchi K, Shimizu Y, Bronson RT, Gao YH, Inada M, Sato M, Okamoto R, et al. Targeted disruption of Cbfa1 results in a complete lack of bone formation owing to maturational arrest of osteoblasts. Cell 1997;89:755–764. [PubMed: 9182763]

Levanon D, Negreanu V, Bernstein Y, Bar-Am I, Avivi L, Groner Y. AML1, AML2, and AML3, the human members of the runt domain gene-family: cDNA structure, expression, and chromosomal localization. Genomics 1994;23:425–432. [PubMed: 7835892]

Levanon D, Bettoun D, Harris-Cerruti C, Woolf E, Negreanu V, Eilam R, Bernstein Y, Goldenberg D, Xiao C, Fliegauf M, Kremer E, Otto F, Brenner O, Lev-Tov A, Groner Y. The Runx3 transcription factor regulates development and survival of TrkC dorsal root ganglia neurons. EMBO J 2002;21:3454–3463. [PubMed: 12093746]

Li QL, Ito K, Sakakura C, Fukamachi H, Inoue K, Chi XZ, Lee KY, Nomura S, Lee CW, Han SB, Kim HM, Kim WJ, Yamamoto H, Yamashita N, Yano T, Ikeda T, Itohara S, Inazawa J, Abe T, Hagiwara A, Yamagishi H, Ooe A, Kaneda A, Sugimura T, Ushijima T, Bae SC, Ito Y. Causal relationship between the loss of RUNX3 expression and gastric cancer. Cell 2002;109:113–124. [PubMed: 11955451]

Mundlos S, Otto F, Mundlos C, Mulliken JB, Aylsworth AS, Albright S, Lindhout D, Cole WG, Henn W, Knoll JH, Owen MJ, Mertelsmann R, Zabel BU, Olsen BR. Mutations involving the transcription factor CBFA1 cause cleidocranial dysplasia. Cell 1997;89:773–779. [PubMed: 9182765]

Nieuwkoop, PD.; Faber, J. Normal table of Xenopus laevis (Daudin). Amsterdam, The Netherlands: North Holland Publishing Company; 1967.

North T, Gu TL, Stacy T, Wang Q, Howard L, Binder M, Marin-Padilla M, Speck NA. Cbfa2 is required for the formation of intra-aortic hematopoietic clusters. Development 1999;126:2563–2575. [PubMed: 10226014]

NIH-PA Author Manuscript

NIH-PA Author Manuscript

NIH-PA Author Manuscript

Okuda T, van Deursen J, Hiebert SW, Grosveld G, Downing JR. AML1, the target of multiple chromosomal translocations in human leukemia, is essential for normal fetal liver hematopoiesis. Cell 1996;84:321–330. [PubMed: 8565077]

Otto F, Thornell AP, Crompton T, Denzel A, Gilmour KC, Rosewell IR, Stamp GW, Beddington RS, Mundlos S, Olsen BR, Selby PB, Owen MJ. Cbfa1, a candidate gene for cleidocranial dysplasia syndrome, is essential for osteoblast differentiation and bone development. Cell 1997;89:765–771. [PubMed: 9182764]

Pearson WR, Robins G, Zhang T. Generalized neighbor-joining: more reliable phylogenetic tree reconstruction. Mol. Biol. Evol 1999;16:806–816. [PubMed: 10368958]

Roberts A. Early functional organization of spinal neurons in developing lower vertebrates. Brain Res. Bull 2000;53:585–593. [PubMed: 11165794]

Sadaghiani B, Thiebaud CH. Neural crest development in the Xenopus laevis embryo, studied by interspecific transplantation and scanning electron microscopy. Dev. Biol 1987;124:91–110. [PubMed: 3666314]

Schlosser G, Northcutt RG. Development of neurogenic placodes in Xenopus laevis. J. Comp. Neur 2000;418:121–146. [PubMed: 10701439]

Speck NA, Gilliland DG. Core-binding factors in haematopoiesis and leukaemia. Nat. Rev. Cancer 2002;2:502–513. [PubMed: 12094236]

Stricker S, Fundele R, Vortkamp A, Mundlos S. Role of Runx genes in chondrocyte differentiation. Dev Biol 2002;245:95–108. [PubMed: 11969258]

Thompson JD, Higgins DG, Gibson TJ. CLUSTAL W: improving the sensitivity of progressive multiple sequence alignment through sequence weighting, position-specific gap penalties and weight matrix choice. Nucleic Acids Res 1994;22:4673–4680. [PubMed: 7984417]

Tracey WD, Pepling ME, Marko EH, Thomsen GH, Gerben JP. A Xenopus homologue of aml-1 reveals unexpected patterning mechanisms leading to the formation of embryonic blood. Development 1998;125:1371–1380. [PubMed: 9502719]

Wang Q, Stacy T, Binder M, Marin-Padilla M, Sharpe AH, Speck NA. Disruption of the Cbfa2 gene causes necrosis and hemorrhaging in the central nervous system and blocks definitive hematopoiesis. Proc. Natl. Acad. Sci. USA 1996;93:3444–3449. [PubMed: 8622955]

Wijmenga C, Speck NA, Dracopoli NC, Hofker MH, Liu P, Collins FS. Identification of a new murine runt domain-containing gene, Cbfa3,and localization of the human homolog, CBFA3, to chromosome 1p35-pter. Genomics 1995;26:611–614. [PubMed: 7607690]

NIH-PA Author Manuscript
NIH-PA Author Manuscript
NIH-PA Author Manuscript

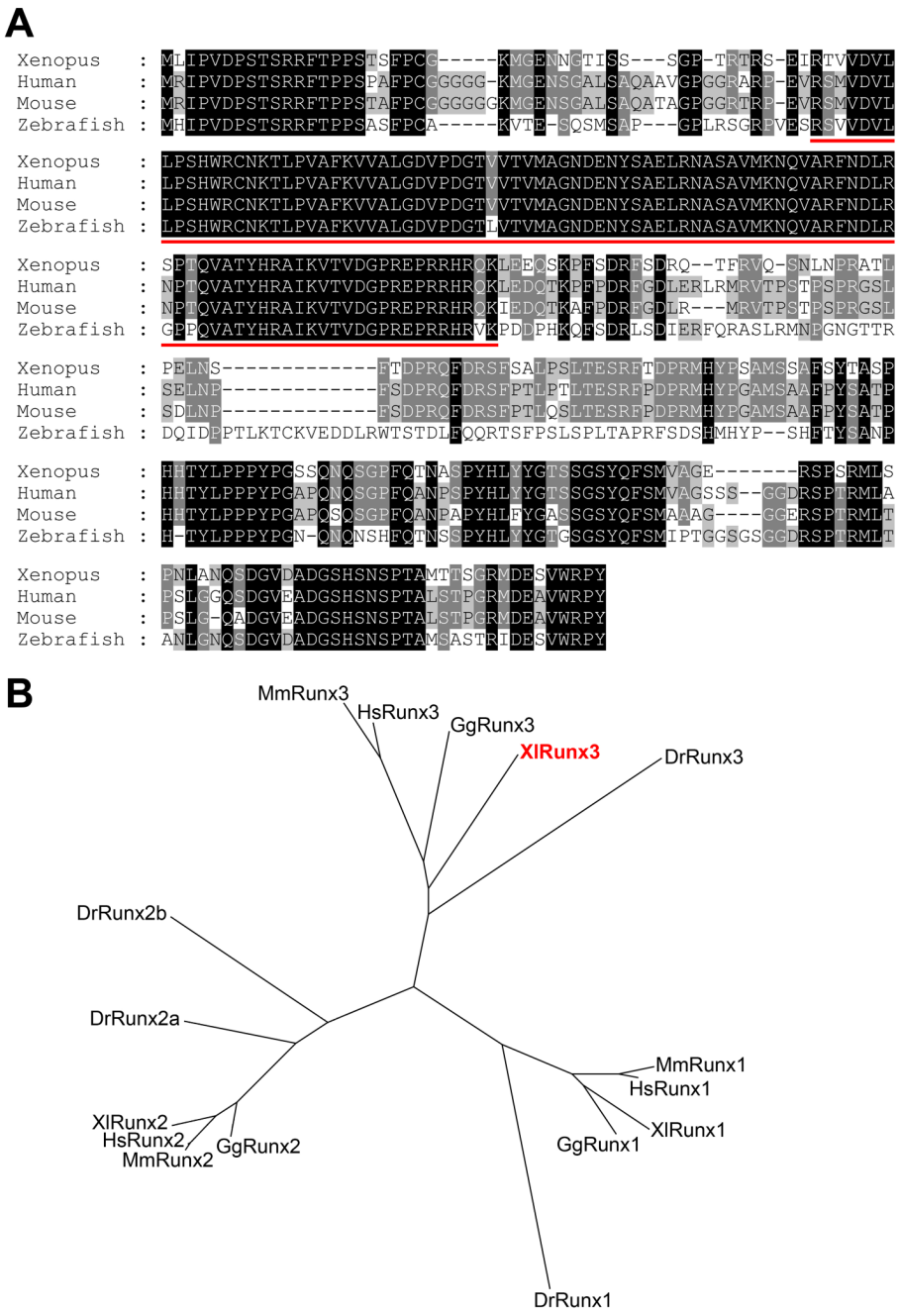

Figure 1. Sequence and structure comparison of Runx3 proteins across species

(A) The predicted amino acid sequences from *Xenopus laevis*, human, mouse and zebrafish *Runx3* were aligned using ClustalW. Conserved amino acids in all four species or in at least two species are highlighted in black and grey, respectively. The Runt domain, signature motif of this class of molecules, is underlined in red. **(B)** Phylogenetic tree analysis of Runx proteins from *Xenopus laevis* (Xl), human (Hs), mouse (Mm), chicken (Gg) and zebrafish (Dr). Accession numbers for the source sequences are indicated in materials and methods.

NIH-PA Author Manuscript

NIH-PA Author Manuscript

NIH-PA Author Manuscript

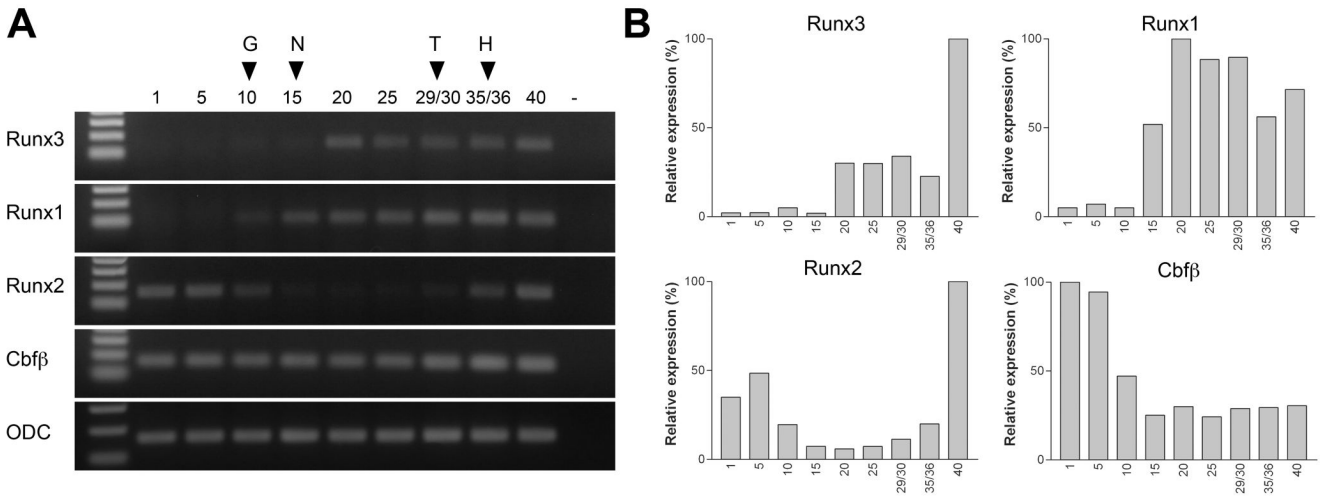

Figure 2. Temporal expression of *Runx3, Runx1, Runx2* and *Cbf*β during embryogenesis

(A) RT-PCR analysis of the developmental expression of *Runx3, Runx1, Runx2 and Cbf*β. Stages are according to Nieuwkoop and Faber (1967). *Ornithine decarboxylase* (*ODC*) is shown as a loading control. G, onset of gastrulation; N, mid-neurula stage; T, tailbud stage; H, hatching stage. **(B)** Real-time RT-PCR analysis of *Runx3, Runx1, Runx2 and Cbf*β. Each value has been normalized to the level of *ODC*.

NIH-PA Author Manuscript
NIH-PA Author Manuscript
NIH-PA Author Manuscript

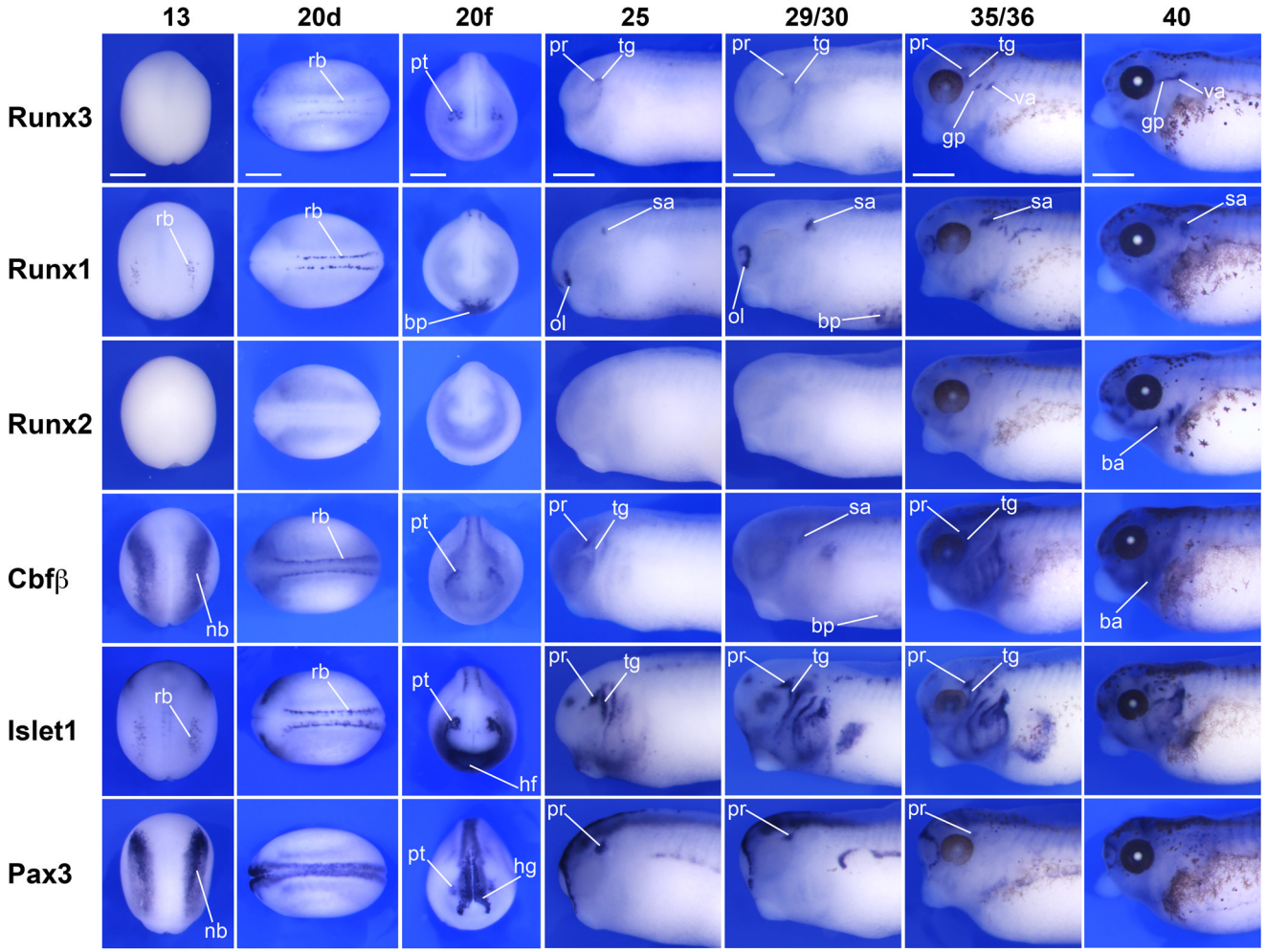

Figure 3. Comparative analysis of the expression of *Runx* and *Cbf*β genes by whole-mount in situ hybridization

Runx3 is first detected at stage 20 in two domains, the developing primary sensory (Rohon-Beard) neurons and the trigeminal-profundal placode. At the same stage *Cbf*β is also co-expressed in both domains, while *Runx1* is restricted to Rohon-Beard neurons. At later stages, stage 25 and up, *Runx3* expression appears to be largely confined to the head region and in a number of cranial nerves including the ganglion of the trigeminal, vagal and glossopharyngeal nerves. To confirm the tissue-specific expression of *Runx* genes, we also performed *in situ* hybridization for *Pax3* and *Islet1* in staged matched embryos. *Pax3* and *Islet1* share common expression domains with *Runx* genes in the profundal-trigeminal placode (*Pax3* and *Islet1*), Rohon-Beard sensory neurons and cranial ganglia (*Islet1*). Stages are according to Nieuwkoop and Faber (1967). Stage 13, dorsal view anterior to top. Stage 20d, dorsal view anterior to the left. Stage 20f, frontal view dorsal to top. Stage 25–40, lateral view of the head region, anterior to the left and dorsal to top. ba, branchial arches region; bp, blood progenitors; hf, heart field; hg, hatching gland; gp, glossopharyngeal; nb, neural plate border; ol, olfactory placode; pr, profundal ganglia; rb, Rohon-Beard neurons; sa, statoaccoustic ganglia; tg, trigeminal ganglia; pt, profundal-trigeminal placode; va, vagal nerve. The scale bars in the upper row represent 500 μm.

NIH-PA Author Manuscript
NIH-PA Author Manuscript
NIH-PA Author Manuscript

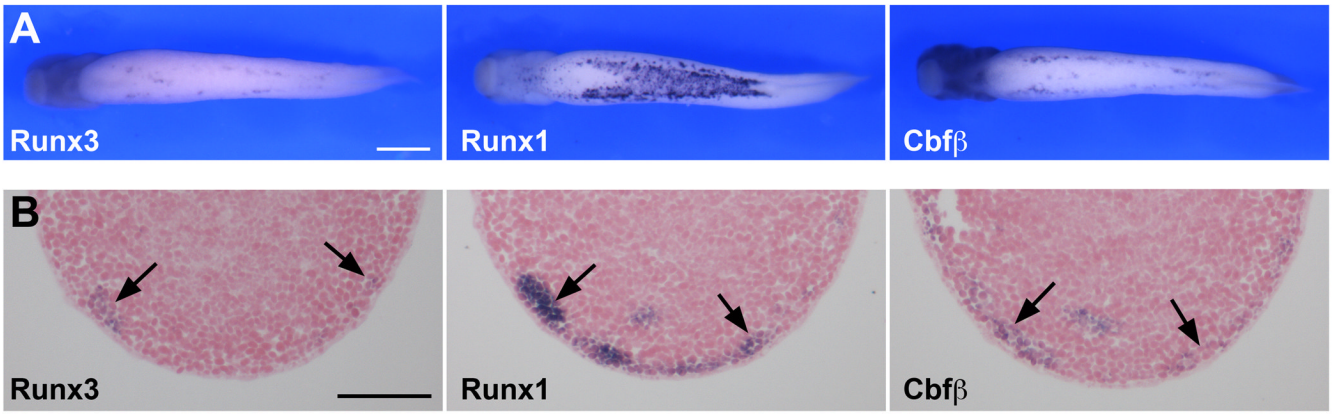

Figure 4. Comparative analysis of *Runx3, Runx1* and *Cbf*β in blood progenitors

(A) Whole-mount *in situ* hybridization of stage 31 embryos viewed from the ventral side, anterior to the left, highlights the expression of *Runx3, Runx1* and *Cbf*β in blood progenitors. In these cells *Runx1* appears to be expressed at higher level than *Runx3* and *Cbf*β. The scale bar represents 500 μm. **(B)** *In situ* hybridization on adjacent sections of a stage 31 embryo shows that Runx3, Runx1 and *Cbf*β expression domain overlap at least in the lateral most aspect of the lateral plate mesoderm (arrows). The scale bar represents 100 μm

NIH-PA Author Manuscript
NIH-PA Author Manuscript
NIH-PA Author Manuscript

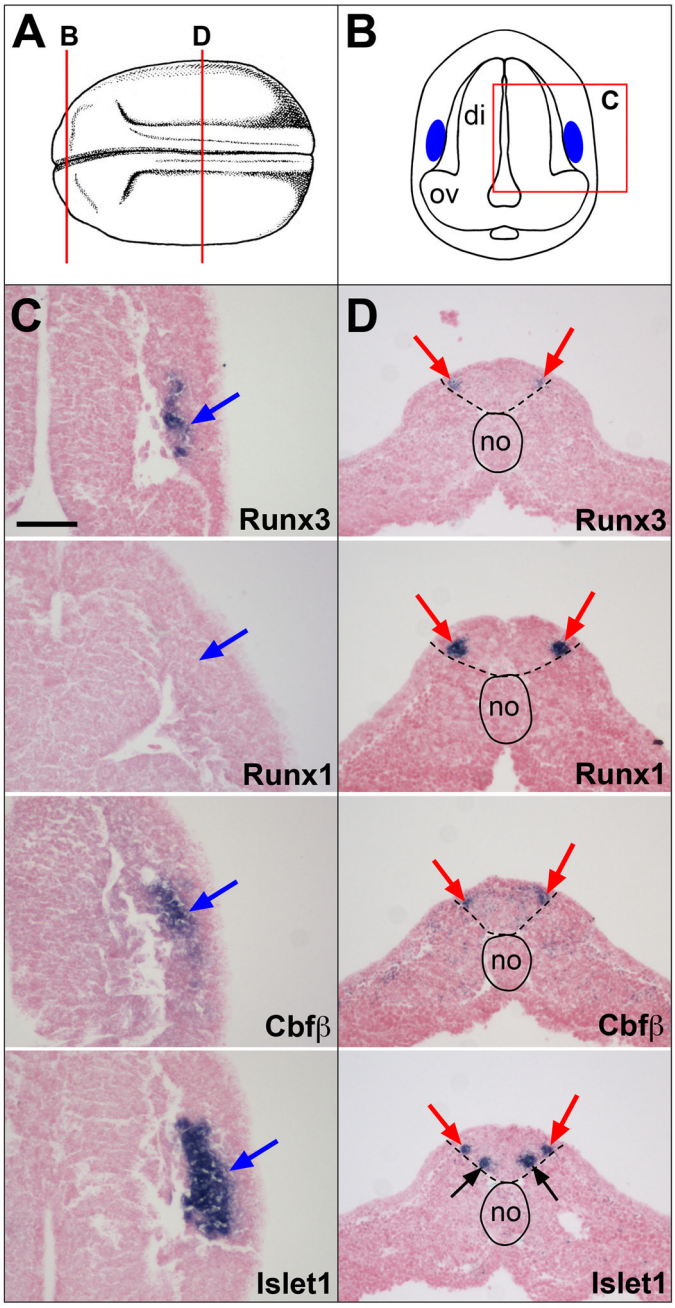

Figure 5. Comparative analysis of *Runx3, Runx1, Cbf*β and *Islet1* expression in the profundal-trigeminal placode and Rohon-Beard sensory neurons at stage 20

(A) Schematic representation of a stage 20 embryo view from the dorsal side, anterior to the left. Modified from Nieuwkoop and Faber (1967). **(B)** Schematic representation of a transverse section at the level of the diencephalon, corresponding to the line labeled “B” in panel (A). Dorsal to top. The blue areas indicate the position of the developing profundal-trigeminal placode. The boxed area labeled “C” is the region of the section shown in subsequent panels (C). **(C)***Runx3*, *Cbf*β and *Islet1* are coexpressed in the profundal-trigeminal placode (blue arrows), while *Runx1* is not detected in this tissue. **(D)** Transverse sections in the trunk region corresponding to the line labeled “D” in panel (A). All four genes are coexpressed in Rohon-

NIH-PA Author Manuscript

NIH-PA Author Manuscript

NIH-PA Author Manuscript

Beard sensory neurons (red arrows). *Islet1* is also expressed in the population of ventral interneurons (black arrows). The notochord is outlined with a solid line, while the position of the neural tube is underlined with dashed lines. The probes are indicated in the lower right corner of each panel. di, diencephalon; no, notochord; ov, optic vesicle. The scale bar in panel C represents 100 μm.

NIH-PA Author Manuscript
NIH-PA Author Manuscript
NIH-PA Author Manuscript

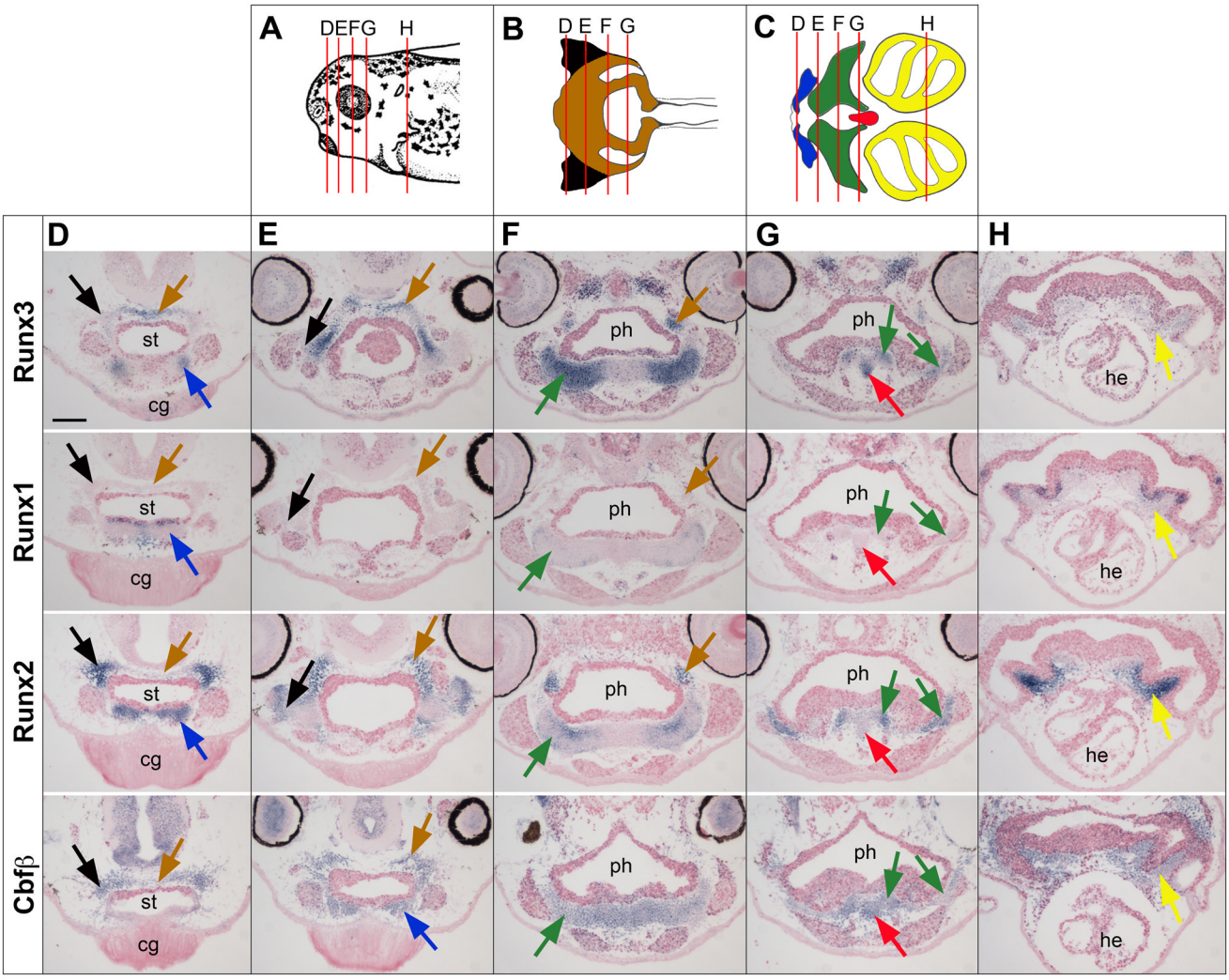

Figure 6. Comparative analysis of *Runx3, Runx1, Runx2* and *Cbf*β expression in the craniofacial cartilage at stage 40

(A) Schematic representation of the head of a stage 40 embryo viewed from the lateral side, dorsal to top, anterior to the left. Modified from Nieuwkoop and Faber (1967). **(B, C)** Schematic representations of the ventral **(B)** and dorsal **(C)** cranial cartilage elements. Modified from Sadaghiani and Thiebaud (1987). The cartilage elements are color-coded: ethmoid-trabecular (brown), quadrate (black), Meckel's (blue), cerathoyal (green), basihyal (red) and branchial (yellow). In panels (A), (B) and (C) the lines labeled "D", "E", "F", "G" and "H" indicate the level of the transverse sections shown in the subsequent panels. cg, cement gland; he, heart; ph, pharynx; st, stomodeum. The scale bar in panel D represents 100 μm.

NIH-PA Author Manuscript
NIH-PA Author Manuscript
NIH-PA Author Manuscript

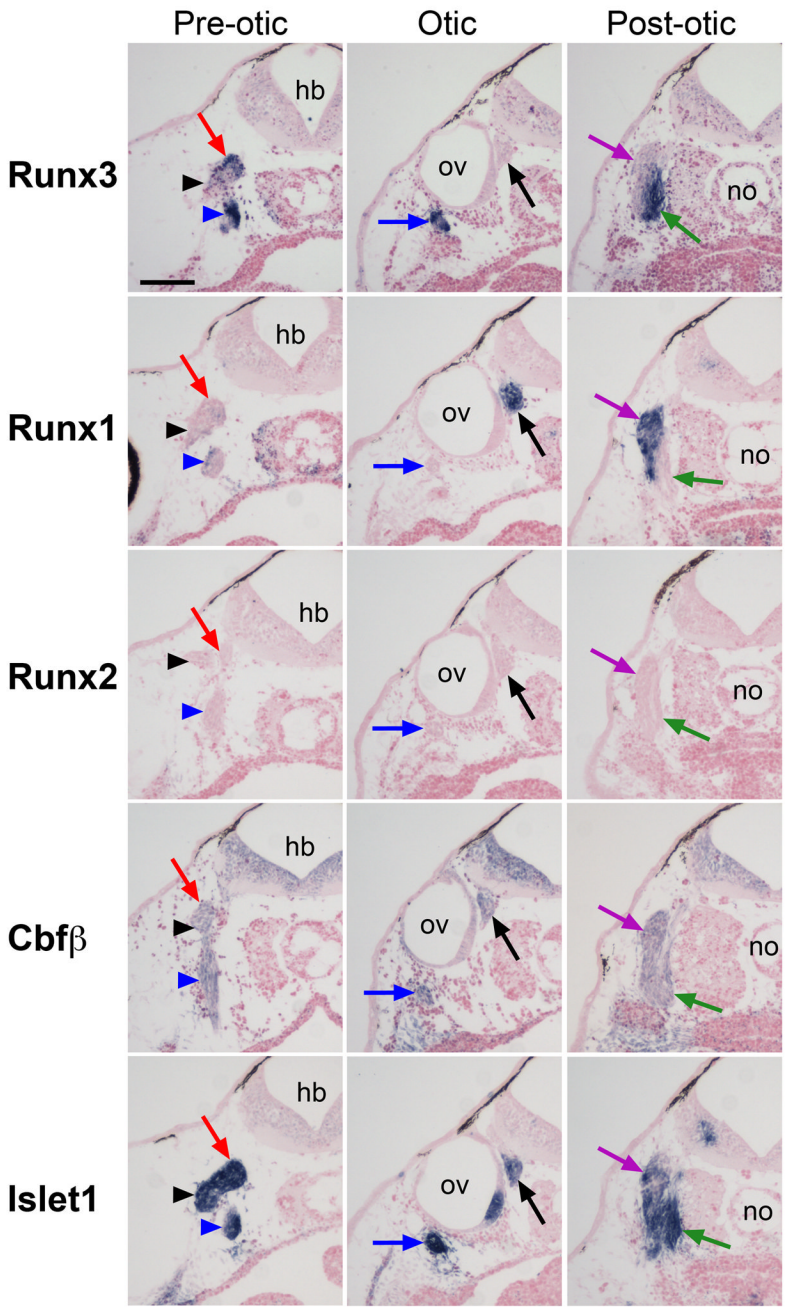

Figure 7. Comparative analysis of *Runx3, Runx1, Runx2, Cbfβ* and *Islet1* expression in neurogenic placode derivatives at stage 40

Transverse sections were performed at three levels along the antero-posterior axis; the pre-otic, the otic, and post-otic regions. Each column shows sections from approximately the same level. Trigeminal ganglion (red arrows), ganglion of anterodorsal lateral line nerve (black arrowheads), ganglia of facial and anteroventral lateral line nerves (blue arrowheads), ganglia of glossopharyngeal and middle lateral line nerves (blue arrows), statoaccoustic ganglion (black arrows), ganglion of vagal nerve (green arrows), ganglion of posterior lateral line nerve (purple arrows). hb, hindbrain; no, notochord; ov, otic vesicle; The scale bar in the upper left panel represents 100 μm.

NIH-PA Author Manuscript
NIH-PA Author Manuscript
NIH-PA Author Manuscript

Table 1

Summary of *Runx1*, *Runx2*, *Runx3*, and *Cbf*β tissues expression during *Xenopus* development

	Runx1	Runx2	Runx3	Cbfβ
Blood progenitors	+	−	+	+
Rohon-Beard sensory neurons	+	−	+	+
Profundal-trigeminal placode	−	−	+	+
Olfactory placode	+	−	−	+
Trigeminal ganglion	−	−	+	+
Ganglion of anterodorsal lateral line nerve	−	−	+/−	+
Ganglia of facial and anteroventral lateral line nerves	−	−	+	+
Statoaccoustic ganglion	+	−	−	+
Ganglia of glossopharyngeal and middle lateral line nerves	−	−	+	+
Ganglion of posterior lateral line nerve	+	−	−	+
Ganglion of vagal nerve	−	−	+	+
Meckel's cartilage	−	+	+	+
Ceratoyal cartilage	+/−	+	+	+
Basihyal cartilage	−	−	+	+
Branchial cartilage	−	+	−	+
Quadrate cartilage	−	+	−	+
Ethmoid-trabecular cartilage	−	+	+	+

"+", gene strongly expressed in the corresponding tissue; "+/−", weakly expressed; "−", undetected.